



ELSEVIER

Journal of Electron Spectroscopy and Related Phenomena 77 (1996) 33–40

**JOURNAL OF
ELECTRON SPECTROSCOPY**
and Related Phenomena

Coherent forward emission (CFE) from adsorbed molecules: ($\sqrt{3} \times \sqrt{3}$)R30° CO/Pd(111) and (2 × 1)CO + O/Pd(111)

H. Geisler^a, J. Wambach^a, H. Kuhlenbeck^{a,*}, H.-J. Freund^a, M. Neuber^b, M. Neumann^b^a*Physikalische Chemie 1, Ruhr-Universität Bochum, Universitätsstraße 150, D-44780 Bochum, Germany*^b*Fachbereich Physik, Universität Osnabrück, Barbarastraße 7, D-49076 Osnabrück, Germany*

Received 2 March 1995; accepted in final form 31 July 1995

Abstract

We report angle resolved valence photoelectron spectra for CO adsorbed on Pd(111) and O/Pd(111) over a photon energy range of 20–250 eV. An oscillatory behaviour of the photoelectron cross sections of the valence electrons in normal emission is found. This is interpreted as being due to the interference of electron waves emitted from different parts of the wavefunctions of the CO valence orbitals. Therefore the oscillations should contain information about the electron distribution in the individual levels and the internuclear spacings of the molecule.

Keywords: Carbon monoxide adsorption; Coherent forward emission; Photoelectron diffraction

1. Introduction

Interference of electron waves plays an important role in the field of spectroscopy. It is the basic mechanism of well established methods such as SEXAFS [1,2], photoelectron diffraction [3] and LEED, and it is also the process which leads to the effect of coherent forward emission (CFE) [4], which has been studied in this work for adsorbed CO molecules.

The basic mechanism of SEXAFS is the creation of an outgoing electron wave through photoexcitation of a core hole. As the wavelength of the outgoing electron wave is changed, the interference between the outgoing and the backscattered wave leads to oscillations of the absorption coefficient. Arguments similar to those for SEXAFS apply to

core level photoelectron diffraction [3]. In the present case, electron waves emitted from valence ion states have been studied. The photoionization cross section as a function of photoelectron energy exhibits an oscillatory behaviour which is caused by coherent forward scattering (CFE: coherent forward emission) of electrons emitted from valence ion states which can be described as superpositions of electron densities localized near to the nuclei of the system. For SEXAFS only one emitting atom has to be considered, whereas for CFE the electron wave is emitted from two centres, which gives rise to additional interference effects (see Fig. 1). In a very simple picture, where the outgoing electron wave is approximated by a superimposition of two free electron waves, CFE leads to an intensity resonance when the bond length is an integer multiple of the electron wavelength (Fig. 2). However, phase shifts,

* Corresponding author.

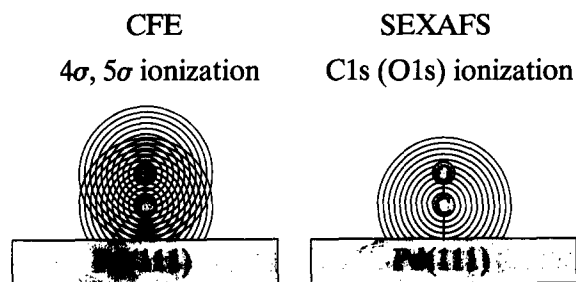


Fig. 1. Schematic illustrations of the outgoing electron waves in CFE and SEXAFS.

scattering of the outgoing wave at neighbouring atoms and the influence of the molecular potential on the wavefunction of the outgoing electron lead to deviations from this simple picture [4].

As pointed out by Gustafsson [4], in CFE the intensities of the oscillations are determined by rather large forward scattering amplitudes and not by the comparatively small back scattering amplitudes as in the case of SEXAFS. As examples to demonstrate the effect, we have studied the adsorbate systems $(\sqrt{3} \times \sqrt{3})R30^\circ$ CO/Pd(111) ($\Theta_{\text{CO}} = 0.33$) and (2×1) CO + O/Pd(111) ($\Theta_{\text{CO}} = 0.5, \Theta_{\text{O}} = 0.5$).

The first studies on the cross section of CO valence levels were undertaken by Shirley et al. [5]. However, only a few data points were taken over a limited range of photon energies, and the first CFE resonance was barely visible.

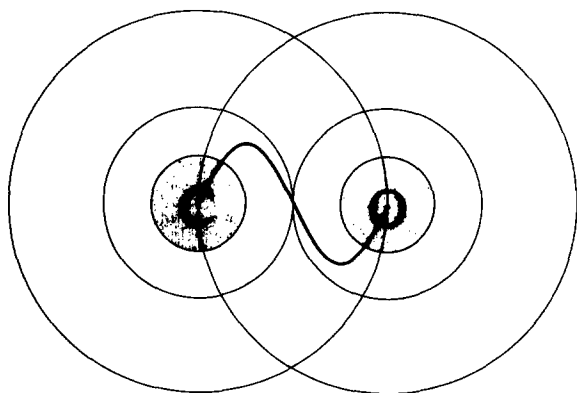


Fig. 2. Schematic drawing of an outgoing electron wave in the first CFE resonance assuming that the emitted partial waves can be approximated by wave functions of free electrons.

2. Experimental

The experiments were performed in an UHV chamber operated at a base pressure better than 10^{-8} Pa. The magnetically shielded chamber was equipped with facilities for angle resolved photoemission with an angular resolution of $\approx 1.5^\circ$, and for LEED, AES, and residual gas analysis. Photoelectron spectra were excited using light from the exit slit of the toroidal grating monochromator TGM2 operated at the electron storage ring BESSY in Berlin (Germany). The beam intensity was monitored by a gold electrode mounted behind the exit slit of the monochromator.

The sample was spot welded to two tungsten wires, which were attached to two tungsten rods. These rods were pressed into two holes in a sapphire block which was connected to a liquid nitrogen reservoir. With this setup, temperatures as low as ≈ 80 K could be reached. For heating purposes a tungsten filament was mounted behind the crystal. It could be used for heating via electron bombardment or heat radiation. The temperature was monitored with a chromel/alumel thermocouple.

Crystal cleaning was performed by repeated cycles of sputtering at $T \approx 600$ K and annealing at $T \approx 1100$ K until LEED and AES indicated a clean and well ordered surface.

The (2×1) CO + O/Pd(111) adsorbate was prepared by admission of 1.5 l of CO at $T \approx 200$ K onto a (2×2) O overlayer. Details of the preparation are given in [6,7].

3. Results and discussion

Fig. 3 shows a set of electron distribution curves as a function of photon energy for $(\sqrt{3} \times \sqrt{3})R30^\circ$ CO/Pd(111). These data were normalized to the photon flux and the intensities were then multiplied by the photon energy. The latter step was necessary in order to enhance the intensities of the structures in the spectra taken at higher photon energy, which would otherwise simply be straight lines in the plots. Therefore these figures provide a rough overview of the raw data, but the resonance maxima appear to be shifted to somewhat higher energies.

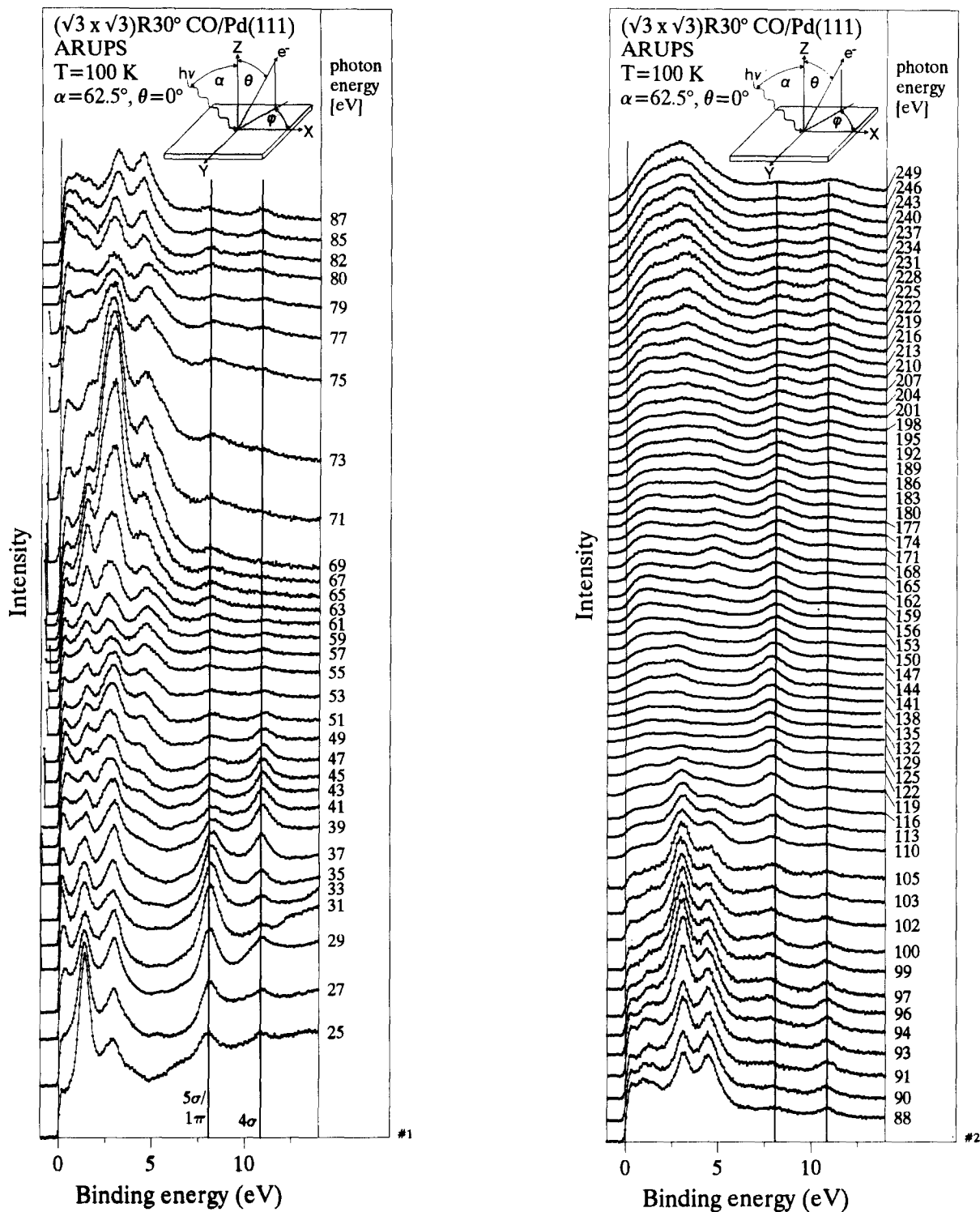


Fig. 3. Photoelectron spectra of $(\sqrt{3} \times \sqrt{3})R30^\circ$ CO/Pd(111) as a function of photon energy.

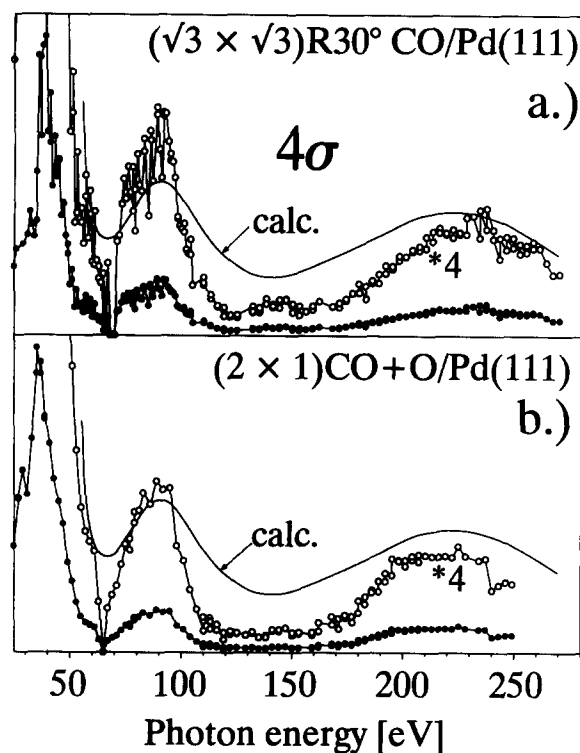


Fig. 4. Intensity of the 4σ level as a function of photon energy of (a) $(\sqrt{3} \times \sqrt{3})R30^\circ$ CO/Pd(111) and (b) (2×1) CO+O/Pd(111). For comparison, results of a calculation performed by Gustafsson for a C–O spacing of 1.13 Å are shown (reproduced from [4]).

Fig. 4 shows the intensities for the 4σ levels in the spectra of the two systems as a function of photon energy. The data have been obtained by integration of the respective peaks after subtraction of the spectra of the clean surfaces. In each case we find the well known strong σ^* shape resonance at energies of ≈ 37 eV and two additional resonances at photon energies of ≈ 85 and 225 eV. The latter maxima are due to coherent forward scattering. Gustafsson pointed out on the basis of $x\alpha$ -SW calculations of oriented CO that the positions of

the maxima in the 4σ photoemission cross section are sensitive to the CO bond length [4]. An extension or reduction of the CO bond length by, for instance, 0.1 Å leads to a shift of the first CFE maximum by ≈ 14 eV and the second one should shift by ≈ 35 eV. Reduction of the bond length leads to a shift to higher or bond extension to a shift to lower photon energy. One may suspect that the σ^* shape resonance at ≈ 37 eV is itself a part of the series of maxima. This is, however, not the case. The latter resonance may be interpreted as being due to the formation of a standing wave between the atoms due to backscattering. This is of course different from the CFE process, where one has to deal with the interference of waves emitted from different centres. Nevertheless, the position of the σ^* shape resonance should at first sight also be a measure of the CO bond length. Its use, however, is not without problems, as the standing wave is strongly influenced by the molecular potential, which may be different for different surroundings of the CO molecules. An extensively discussed example is the shift of the σ^* shape resonance upon coadsorption of Na [8–10]. For the $4\sigma \rightarrow \sigma^*$ resonance the shift is small, pointing towards a negligible elongation of the bond length [8], whereas the shape resonance shifts significantly in NEXAFS [9,10], where excitations of core electrons are probed. The latter type of shift has been used in the past to deduce a strong elongation of the CO bond upon coadsorption of Na.

The positions of the 4σ resonance maxima as obtained from the data shown in Fig. 4 are listed in Table 1. From these data the bond lengths, which are also given in Table 1, have been estimated from data published by Gustafsson [4] for gas phase CO molecules. Using the $x\alpha$ -SW method, he calculated the 4σ cross section as a function of photon energy for bond lengths of 1.24, 1.13 and 1.02 Å, with the second value

Table 1

4σ resonance energies for the studied adsorbate systems (photon energies). The given bond lengths have been estimated from calculated data for gas phase CO molecules [4]

Adsorbate	Shape resonance	1. CFE resonance	2. CFE resonance	ΔE_{CFE}	Bond length
$\sqrt{3} \times \sqrt{3})R30^\circ$ CO	39 ± 3 eV	85 ± 5 eV	225 ± 8 eV	140 eV	1.11 ± 0.06 eV
(2×1) CO + O	37 ± 3 eV	85 ± 5 eV	215 ± 8 eV	130 eV	1.15 ± 0.06 eV

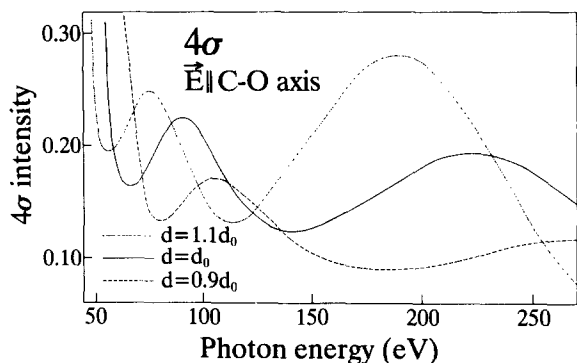


Fig. 5. Calculated intensities of the 4σ level as a function of photon energy for three different C–O bond lengths. Reproduced from [4].

being the bond length of an undisturbed CO molecule in the gas phase (see Fig. 5). The positions of the calculated resonance maxima and their energetic spacings are listed in Table 2. As the absolute positions of the experimentally determined CFE resonances as listed in Table 1 only approximately obeyed the law for the positions of the two resonances as derived from Gustafsson's calculations, we estimated the given bond lengths from the energetic spacings of the two resonances instead of using their absolute positions.

The estimated C–O bond length for the pure adsorbate is in good agreement with the result obtained by Ohtani et al. [11] using LEED. They found that the C–O distance for $(\sqrt{3} \times \sqrt{3})R30^\circ$ CO/Pd(111) should be 1.15 ± 0.05 Å. Considering the given error bars, this agrees well with our result of 1.11 ± 0.06 Å.

The data of Gustafsson [4] (see Fig. 5 and Table 2) show that the positions of the resonance maxima should be very sensitive towards a change of the bond length, so that significant changes should be easily detectable. From the data listed in Table 1 it is obvious that coadsorption of oxygen does not

Table 2
Positions of the CFE resonances of the 4σ level as obtained from Fig. 5 [4]

Bond length	1. CFE resonance	2. CFE resonance	ΔE
1.24 Å	75 eV	188 eV	113 eV
1.13 Å	89 eV	225 eV	136 eV
1.02 Å	105 eV	≈ 260 eV	≈ 155 eV

lead to a notable change of the C–O bond length; only a slight extension of the C–O distance seems to occur, which is still within the error bars.

In a simple picture one would expect a contraction of the C–O bond length upon coadsorption of oxygen, since the oxygen atoms should be negatively charged, thereby removing electron density from their surroundings. This in turn should diminish the occupation of the $2\pi^*$ level of the CO molecules. As this level is antibonding, one would expect a reduced C–O bond length. This model is, however, rather simple and therefore it does not necessarily lead to the correct conclusions.

Contrary to the simple model presented above, the results of this study point towards a slight extension of the C–O bond length. It is, however, not clear whether this result is significant, as the absolute value of the extension is within the error bars imposed upon our results from the errors in determination of the positions of the resonance maxima. An additional error is introduced by the fact that Gustafsson's calculations were performed for isolated CO molecules, neglecting modifications of the wavefunctions of the CO molecules due to interaction with the substrate, the other adsorbed CO molecules and coadsorbed molecules, if present. Also, scattering of the outgoing electron wave at the Pd substrate is not considered in the calculations.

There has been a certain interest in this adsorbate system in the past, as CO on Pd(111) may be oxidized to CO_2 by coadsorbed oxygen and CO_2 may be dissociated into $\text{CO} + \text{O}$ [12]. This interest has led to several publications [6,7,13,14]. Since the density of the adsorbate on the surface is rather high, it was expected that the properties of the CO molecules would be modified with respect to those of the pure CO adsorbate. However, a recent ARUPS study did not show evidence of any considerable modification of the properties of the CO molecules upon coadsorption of oxygen [7]. This is also documented in the weak influence of coadsorbed oxygen on the spectra of the CO adsorbate. Only small variations of the valence level binding energies are observed, i.e. 0.15 eV for the $5\sigma/17\pi$ level and 0.27 eV for the 4σ emission (see Fig. 6). Therefore the result obtained in this study is in line with the result of the previous study.

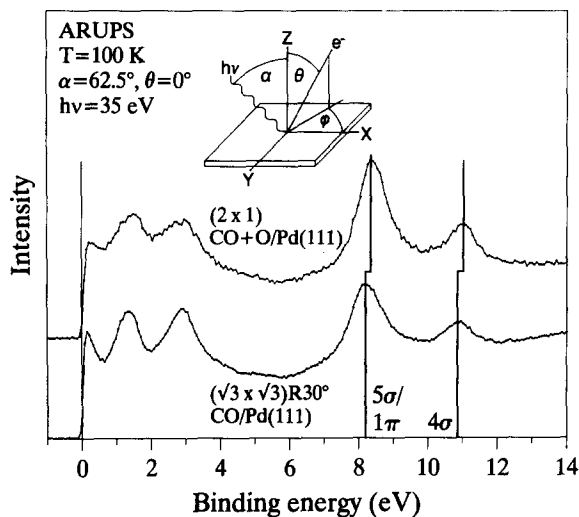


Fig. 6. Comparison of ARUPS spectra of $(\sqrt{3} \times \sqrt{3})R30^\circ$ CO/Pd(111) and (2×1) CO + /Pd(111).

In addition to the already discussed CFE resonances, the 4σ cross sections of the systems studied exhibit a small maximum at ≈ 140 eV. The origin of this feature is not yet clear. We consider two possible reasons. Firstly, it could be due to interference of the outgoing electron wave with intensity scattered back from the substrate. The distance corresponding to this resonance may then be estimated assuming that the wavelength of the outgoing electron is twice the unknown distance, similar to the case of the first SEXAFS resonance, neglecting any effects of phase shifts and damping. From this one obtains the result that the unknown distance should be ≈ 0.5 Å, which is too small to be an existing distance in the adsorbate system. Of course, SEXAFS resonances of higher order could also be considered, which would lead to larger distances, so that one would finally reach a value which might be near to an existing distance. The second possibility is that the feature is a shape resonance of third order. This may be tested by exploiting the functional dependence of the resonance energy on the electron wavelength. Neglecting phase shifts and approximating the outgoing electron wave by a superposition of two free electron waves emitted from the two centres of the molecule leads to the following equation for the energies of the

Table 3

Values of n for different resonances. For details see text

Resonance	n
1st shape resonance	1/2
2nd shape resonance, 1st CFE resonance	1
3rd shape resonance	3/2
4th shape resonance, 2nd CFE resonance	2

resonance maxima

$$\sqrt{E_{\text{Res}}} = \sqrt{\frac{\hbar^2}{2m_e}} \frac{n}{d} \quad (1)$$

At resonance the C–O bond length d is a multiple of the electron wavelength λ , $d = n\lambda$. The values of n for the different resonances are listed in Table 3.

Fig. 7 shows a plot of the resonance energies as a function of n according to Eq. (1). It is obvious that the experimental values are well described by a linear function as demanded by Eq. (1). However, it is also obvious that Eq. (1) does not adequately describe the real situation, since in this case the line should pass through the origin of the coordinate system. This is not the case, showing that the deviation of the outgoing electron wave from an undisturbed free electron wave is not negligible. Nevertheless, as shown in Fig. 7, all data points are well described by one straight line, which

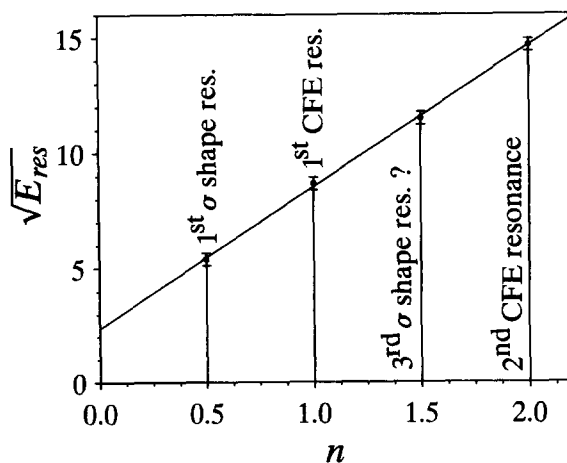


Fig. 7. Square roots of the energies of the different observed 4σ cross section resonances as a function of n for $(\sqrt{3} \times \sqrt{3})R30^\circ$ CO/Pd(111).

gives a rather high probability to the assignment of the intensity maximum at 140 eV to the third σ^* shape resonance.

Finally, we would like to discuss briefly the intensity behaviour of the $5\sigma/1\pi$ peak. The data are shown in Fig. 8.

Apart from the σ^* shape resonance of the 5σ level at ≈ 32 eV, the plots exhibit much less structure than the corresponding plots for the 4σ level (Fig. 4). This is not unexpected: contrary to the case of the 4σ level, for the 5σ level the main intensity is directed towards the substrate, as indicated by the electron density distribution of the orbital [15,16]. A maximum which may be due to the first CFE resonance is found at ≈ 70 eV. At higher energies a broad maximum with some fine structure dominates the spectrum. The fine structure seems to be at least partly significant because it is found in the data of both studied adsorbate systems (see dashed lines). Since for the 5σ level the main emission intensity is directed towards

the substrate, this structure most likely has its origin in the molecular CFE resonances, σ^* shape resonances and maxima due to interference of the outgoing electron wave with intensity scattered back from the substrate.

4. Summary

We have presented data for the intensities of the valence levels of CO in the adsorbate systems $(\sqrt{3} \times \sqrt{3})R30^\circ$ CO/Pd(111) and (2×1) CO + O/Pd(111) over a wide range of photon energies (20–250 eV). For the 4σ level, we find characteristic intensity modulations which are caused by coherent forward emission (CFE), as proposed by Gustafsson [4], and σ^* shape resonances. As the resonance energies depend on the C–O bond length, we were able to provide estimates for this quantity which resulted in the conclusion that coadsorption of oxygen does not change the C–O distance significantly. For the pure $(\sqrt{3} \times \sqrt{3})R30^\circ$ CO/Pd(111) adsorbate the obtained bond length of 1.11 ± 0.06 Å is in good agreement with literature data [11].

In addition to the CFE resonances and the well known shape resonance at ≈ 37 eV, we were able to identify another intensity maximum between the first and the second CFE resonance which we identified as a shape resonance of third order.

Acknowledgements

We thank the Bundesministerium für Forschung und Technologie (BMFT), the Deutsche Forschungsgemeinschaft (DFG) and the Ministerium für Forschung und Technologie des Landes Nordrhein-Westfalen for financial support. H.J.F. also gratefully acknowledges financial help from the Fonds der Chemischen Industrie (FCI).

References

- [1] P.H. Citrin, Surf. Sci., 299/300 (1994) 199.
- [2] P.A. Lee, P.H. Citrin, P. Eisenberger and B.M. Kincaid, Rev. Mod. Phys., 53 (1981) 769.

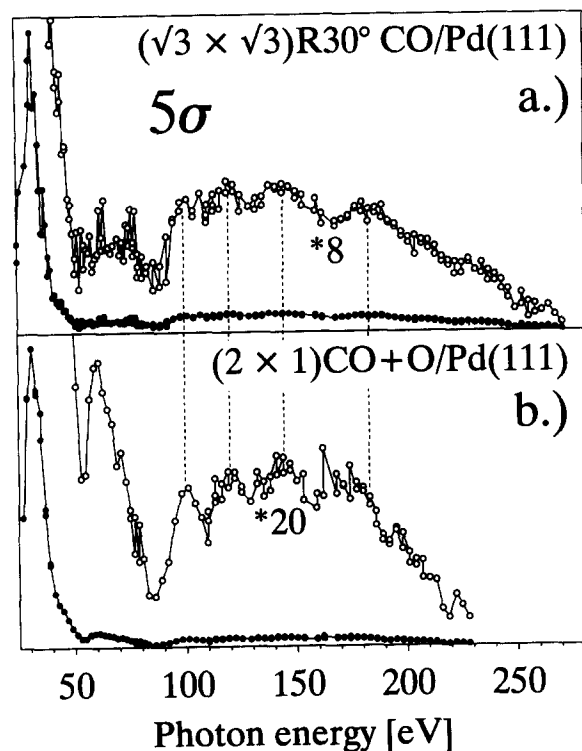


Fig. 8. Intensity of the 5σ level as a function of photon energy of (a) $(\sqrt{3} \times \sqrt{3})R30^\circ$ CO/Pd(111) and (b) (2×1) CO + O/Pd(111).

- [3] M.E. Davila, M.C. Asensio, D.P. Woodruff, K.M. Schindler, P. Hofmann, K.U. Weiss, R. Dippel, V. Fritsche, A.M. Bradshaw, J.C. Comsa and A.R. Gonzales-Elipe, *Surf. Sci.*, 331 (1994) 337.
- [4] T. Gustafsson, *Surf. Sci.*, 94 (1980) 593.
- [5] D.A. Shirley, J. Stöhr, P.S. Weliner, R.S. Williams and G. Apai, *Phys. Scr.*, 16 (1977) 398.
- [6] H. Geisler, Ph.D. Thesis, Ruhr-Universität Bochum, 1994.
- [7] G. Odörfer, E.W. Plummer, H.-J. Freund, H. Kuhlenbeck and M. Neumann, *Surf. Sci.*, 198 (1988) 331.
- [8] G. Paolucci, M. Surman, K.C. Prince, L. Sorba, A.M. McConville and D.P. Woodruff, *Phys. Rev. B*, 34 (1986) 1340.
- [9] J. Stöhr, *NEXAFS Spectroscopy*, Vol. 25 of Springer Series in Surface Sciences, Springer Verlag, Berlin, 1992.
- [10] F. Sette, J. Stöhr, E.B. Kollin, D.J. Dwyer, J.L. Gland, J.L. Robbins and A.L. Johnson, *Phys. Rev. Lett.*, 54 (1985) 935.
- [11] H. Ohtani, M.A. van Hove and G.A. Somorjai, *Surf. Sci.*, 187 (1987) 372.
- [12] D.E. Peebles, D.W. Goodman and J.M. White, *J. Phys. Chem.*, 87 (1983) 4378.
- [13] H. Conrad, G. Ertl and J. Küppers, *Surf. Sci.*, 76 (1978) 323.
- [14] T. Matsushima and H. Asada, *J. Chem. Phys.*, 85 (1986) 1658.
- [15] J.W. Davenport, *Phys. Rev. Lett.*, 36 (1976) 945.
- [16] J.W. Davenport, Ph.D. University Thesis, University of Pennsylvania, 1976.